# EVIDENCE FOR EXCITATION OF POLAR MOTION BY THE FORTNIGHTLY OCEAN TIDES

Richard S. Gross, Kar[illegible] [illegible]amdan, and Dale [illegible] Boggs

Space Geodetic Science and Applications Group
Jet Propulsion Laboratory
California Institute of Technology
Pasadena, California 91109-8099

Corresponding Author:

Richard S. Gross
Jet Propulsion Laboratory
Mail Stop 238-332
4800 Oak Grove Drive
Pasadena, CA 91109-8099, USA
phone: (818) 354-4010
fax: (818) 393-6890
rsg@logos.jpl.nasa.gov

Thursday, November 2, 1995

To be submitted to *Geophysical Research Letters*

# EVIDENCE FOR EXCITATION OF POLAR MOTION BY THE FORTNIGHTLY OCEAN TIDES

by

Richard S. Gross, Karen H. Hamdan, and Dale H. Boggs

Space Geodetic Science and Applications Group
Jet Propulsion Laboratory, California Institute of Technology

**Abstract.** The second-degree zonal tide raising potential, which is responsible for tidal changes in the Earth's rotation rate and length-of-day, is symmetric about the polar axis and hence can excite the Earth's polar motion only through its action upon nonaxisymmetric features of the Earth such as the oceans. Ocean tidal excitation of polar motion in the diurnal and semidiurnal tidal bands has been previously detected and extensively examined. Here, the detection of ocean tidal excitation of polar motion in the long-period tidal band, specifically at the *Mf'* (13.63-day) and *Mf* (13.66-day) tidal frequencies, is reported. Spectra of the SPACE94 polar motion excitation function exhibit peaks at the prograde and retrograde fortnightly tidal periods. After removing the effects of atmospheric wind and pressure changes, an empirical model for the effect of the fortnightly ocean tides upon polar motion excitation is obtained by least-squares fitting periodic terms at the *Mf* and *Mf'* tidal frequencies to the residual polar motion excitation series. SPACE94, a Kalman filter-based combination of space-geodetic measurements of the Earth's rotation spanning 1976.8 - 1994, was chosen for this purpose since its time span is great enough to resolve the *Mf* and *Mf'* tidal frequencies (whose beat period is 18.6 years). The resulting empirical model for the effect of the fortnightly ocean tides upon polar motion excitation, which fully accounts for the observed enhanced power in the fortnightly tidal bands, is compared with the predictions of two hydrodynamic ocean tide models. The models disagree both with each other, with predicted phases differing by 45° to 64° and amplitudes differing by 19 to 27 percent, and with the observations, with both models predicting amplitudes that are generally too small by a factor of two to three. These results illustrate the need for better predictions of the effect of long-period

ocean tides upon the Earth's rotation, a need that may be fulfilled when long-period ocean tide models based upon Topex/Poseidon measurements become available.

## Introduction

The rotation of the solid Earth is not steady but exhibits changes in both: (1) angular speed, giving rise to changes in the length-of-day, and (2) the orientation of the rotation axis within the solid Earth, giving rise to the Earth's polar motion [e.g., *Munk and MacDonald*, 1960; *Lambeck*, 1980, 1988; *Moritz and Mueller*, 1988; *Eubanks*, 1993]. These changes in the rotation of the solid Earth are caused either by: (1) the action of surface forces applied at the solid Earth's interface with its overlying atmosphere and hydrosphere or underlying liquid core, or by (2) changes in the mass distribution of the solid Earth thereby changing its inertia tensor and hence rotation. The tide raising potential due to the gravitational attraction of the sun, Moon, and planets generates deformations of both the oceans, giving rise to the ocean tides, and the solid Earth, giving rise to the body tides. These tidally induced changes in the mass distribution of the oceans and solid Earth, and hence in the Earth's inertia tensor, cause periodic changes in the Earth's rotation at the tidal frequencies.

Changes in the length-of-day caused by the deformation of the solid Earth due to the long-period body tides can be accurately predicted from models of the solid Earth's elastic response to the tide raising potential [*Yoder et al.*, 1981]. The ocean tides contribute to the tidally induced changes in the length-of-day at long periods [*Yoder et al.*, 1981], and because the oceans are asymmetrically located on the surface of the Earth they also generate short-period (diurnal and semidiurnal) length-of-day changes, as well as periodic polar motions. Diurnal and semidiurnal changes in length-of-day and polar motion have been recently detected and attributed to the effects of ocean tides [*Brosche et al.*, 1989, 1991; *Herring and Dong*, 1991, 1994; *Lichten et al.*, 1992; *Wünsch and Busshoff*, 1992; *Wünsch and Seiler*, 1992; *Dickman*, 1993; *Gross*, 1993a; *Herring*, 1993; *Sovers et al.*, 1993; *Brosche and Wünsch*, 1994; *Freedman et al.*, 1994a; *Ray et al.*, 1994;

*Watkins and Eanes*, 1994; *Chao et al.*, 1995]. In this report, evidence is presented for the excitation of polar motion by long-period ocean tides.

## Detection of Fortnightly Polar Motion Excitation Signal

### Polar Motion Excitation Series

The polar motion excitation data set used in this study is that derived from the SPACE94 Earth orientation series. SPACE94 [*Gross*, 1995] is a Kalman filter-based combination of independent Earth orientation measurements taken by the space-geodetic techniques of lunar laser ranging, satellite laser ranging, very long baseline interferometry, and the global positioning system. The Kalman filter used in generating SPACE94 contains a model of the polar motion process and produces estimates of the Earth orientation excitation functions and associated model parameters along with estimates of polar motion and UT1-TAI [*Morabito et al.*, 1988; *Freedman et al.*, 1994b]. The complex-valued polar motion excitation function, or chi-function, is the polar motion forcing function which, at frequencies far from the Free Core Nutation resonance, is related to polar motion through the expression [*e.g.*, *Barnes et al.*, 1983; *Brzezinski*, 1992; *Gross*, 1992; *Brzezinski and Capitaine*, 1993]:

$$\mathbf{p}(t) + \frac{i}{\sigma_{cw}} \frac{d\mathbf{p}(t)}{dt} = \chi(t) \tag{1}$$

where $\mathbf{p}(t) = p_1(t) - i\, p_2(t)$ where $p_1(t)$ and $p_2(t)$ are the x- and y-components, respectively, of polar motion with the positive $p_1$ direction being along the Greenwich meridian and the positive $p_2$ direction being along the meridian at 90° W longitude, $\chi(t) = \chi_1(t) + i\, \chi_2(t)$ where $\chi_1(t)$ and $\chi_2(t)$ are the x- and y-components, respectively, of the polar motion excitation function with the positive $\chi_1$ direction being along the Greenwich meridian and the positive $\chi_2$ direction being along the meridian at 90° E longitude, and $\sigma_{cw}$ is the complex-valued frequency of the Chandler wobble. The polar motion excitation function $\chi(t)$ changes as angular momentum is exchanged with the solid Earth, or as the solid Earth's inertia tensor changes, due to the action of some astronomical or geophysical process such as ocean tides. The path of the pole, given by $\mathbf{p}(t)$ and which is observed by the Earth orientation measurement systems, then responds to this changing excitation function in accordance with equation (1).

The SPACE94 polar motion excitation series consists of 6688 daily values of $\chi(t)$ spanning October 6, 1976 to January 27, 1995. A power spectrum of the first 6656 values of this series, spanning 1976.8–1994, is displayed in Figure 1a where the vertical dotted lines indicate frequencies in the weekly (9-day), fortnightly (14-day), and monthly (27-day) tidal bands. As can be seen, there appears to be enhanced power in the prograde and retrograde fortnightly tidal bands, and perhaps the prograde weekly tidal band. Figure 2a displays a power spectrum of that subset of the SPACE94 polar motion excitation series spanning 1984–1994 where it is again seen that enhanced power is evident in the prograde and retrograde fortnightly and prograde weekly tidal bands.

**Atmospheric Angular Momentum Series**

Significant sources of non-tidal excitation of polar motion should be removed from the SPACE94 excitation series prior to analyzing it for the presence of tidal excitation. There is a growing body of evidence that atmospheric wind and pressure fluctuations are an important excitation mechanism of polar motion at the periods of interest to this study, namely, from a week to a month [*Eubanks et al.*, 1988; *Salstein and Rosen*, 1989; *Nastula et al.*, 1990; *Gross and Lindqwister*, 1992a, 1992b; *Chao*, 1993; *Kuehne et al.*, 1993; *Nastula*, 1992, 1995; *Kosek et al.*, **1995]**. The available atmospheric angular momentum (AAM) series are therefore considered here for possible removal from the SPACE94 polar motion excitation series prior to its analysis for ocean tidal excitation.

Of the AAM data sets currently available, the one with the greatest time span, and the only one that fully overlaps in time with the SPACE94 polar motion excitation series, is that determined from the global analyses produced under the global data assimilation system of the U.S. National Centers for Environmental Prediction (NCEP, formerly the U.S. National Meteorological Center; *McPherson et al.*, 1979; *Kistler and Parrish*, 1982; *Dey and Morone*, 1985; *Kanamitsu*, 1989;

*Kalnay et al.*, 1990). The NCEP AAM values are computed and archived by the International Earth Rotation Service (IERS) Sub-bureau for Atmospheric Angular Momentum (SBAAM) operated by the Climate Prediction Center of the NCEP [*Salstein et al.*, 1993] from which the values used in this study were obtained.

The angular momentum of the atmosphere changes due to both: (1) changes in the strength and direction of the winds, and (2) changes in the atmospheric mass distribution as evidenced by changes in the surface pressure. Furthermore, when computing the AAM pressure term, two different assumptions are usually made about the response of the oceans to the imposed atmospheric pressure changes: (1) the oceans are assumed to respond as an inverted barometer in which case only the mean pressure over the world's oceans is transmitted to the underlying oceanic crust, or (2) the oceans are assumed to be "rigid" thereby fully transmitting the imposed atmospheric pressure variations to the ocean bottom crust. At the periods of interest to this study (a week to a month) the oceans are generally believed to respond as an inverted barometer [*Wunsch*, 1972, 1991; *Brink*, 1978; *Dickman*, 1988a; *Ponte et al.*, 1991; *Ponte*, 1992, 1993, 1994; *Tai*, 1993; *Fu and Pihos*, 1994] and hence this version of the pressure term was chosen for use here.

The AAM values used in this study are diagnostic variables computed from the output of an atmospheric general circulation model (GCM) operated for the primary purpose of forecasting the weather. Changes are often made to the GCM, either to the physical model itself, its representation or parameterization, or to the data being assimilated, in order to improve the weather forecasts. These model changes also lead to improved AAM values, but have the undesired effect of sometimes causing sudden, step-like changes in the mean AAM value, especially of the pressure term, at the time of the model change. These step-like changes in the mean value of the AAM pressure term have been removed [*Dong*, personal communication, 1995] by adjusting the values prior to the occurrence of the model change by applying a constant correction determined from the offset at the time of the model change of smoothing splines fit to the residual AAM values on either side of the step-like change, where the residual AAM series was formed by differencing the NCEP values with those of an independent series computed from the analyses of the GCM operated by the Japan Meteorological Agency (whose AAM values were also obtained from the IERS SBAAM).

After correcting the AAhl pressure term for the effects of model changes, missing values in the pressure and wind terms were filled by linear interpolation. Values for the NCEP AAM wind term are given once-per-day at 0 UT from July 1, 1976 through August 29, 1983, twice-Jmr-day at O UT and 12 UT from August 30, 1983 through June 20, 1992, and four-times-per-day at 0 UT, 6 UT, 12 UT, and 18 UT from June 21, 1992 to the present. Values for the NCEP AAM pressure term computed under the inverted barometer assumption are given once-per-day at 0 UT from July ], 1976 through l>cc.ember 31, 1980, twice-per-day at o UT and 12 UT from January J, 1981 through June 20, 1992, and four-times-per-day at O UT, 6111', 1? UT, and 18 UT from June 21, ] 992 to the present. Because of the diurnal and semidiurnal variations in atmospheric pressure and wind, and hence in the A AM pressure and wind terms, a missing AAM value was replaced by linearly interpolating between the nearest values on either side of the data gap that are given at the same hour (e.g., 12 UT) as that of the missing value. In this manner, data gaps are filled by linear interpolation of values that arc at the same phase in the diurnal and semidiurnal cycles as are the missing values.

After separately filling the gaps in the wind and pressure terms, the total atmospheric angular momentum values were formed by taking their sum. Daily averages of the total A AM values were then formed by averaging the twice-per-day values given from August 30, 1983 through June 20, 1992 and the four-times-per-day values given since June 21, 1992. This is done in order to both: (1) appropriately compare the AAM values to the SPACE94 polar motion excitation values which can be considered to be daily averages since the polar motion observations upon which the SPACE94 excitation series is based are generally daily or multiday average.s, and (2) avoid possible aliasing to long periods of nearly diurnal or nearly semidiurnal AAM variations that would occur if once-]pr-day AAM values given at just, say, 0 UT were chosen for this study. Figure 3 displays the x- and y-components of the daily averaged total AAM time series thus formed. As can be seen, the values prior to about 1984 exhibit greater variability than do the later values, with the values after about 1984 appearing to be more self-consistent.

Figure 1b displays the power spectrum of the residual series formed by subtracting the AAM series shown in Figure 3 from the SPACE94 polar motion excitation series during 1976.8-1994. Enhanced power is still evident in the prograde and retrograde fortnightly tidal bands, but is no longer evident in the prograde weekly tidal band (compare with Figure 1a). The enhanced power in the prograde and retrograde fortnightly tidal bands is particularly evident in Figure 2b which displays a spectrum of that portion of the residual series spanning 1984-1994.

**Determination of an Empirical Tide Model**

In principle, ocean tidal sea level height and current changes at all tidal frequencies are capable of exciting polar motion, but in practice only the largest tides are likely to excite the polar motion to observable levels. In the weekly tidal band the largest ocean tides are the *M9'* (9.12-day) and *M9* (9.13-day) tides, in the fortnightly tidal band they are the *Mf'* (13.63-day) and *Mf* (13.66-day) tides, in the monthly band it is the *Mm* (27.55-day) tide, in the semiannual band it is the *Ssa* (182.62-day) tide, and in the annual band it is the *Sa* (365.26-day) tide. The small difference between the *Mf'* and *Mf* tidal frequencies corresponds to a beat period of 18.6 years, which is also the beat period between the *M9'* and *M9* tidal frequencies. If polar motion excitation effects at these tidal frequencies are to be resolved, then a polar motion excitation time series spanning about 18.6 years must be analyzed. The entire SPACE94-AAM residual polar motion excitation series, spanning the 18.2 year-long interval of 1976.8-1994, was therefore used when fitting for periodic terms at these tidal frequencies.

Besides fitting for periodic terms at the tidal frequencies listed in Table 1, the least-squares fit to the entire SPACE94-AAM residual polar motion excitation series also included terms for the mean and trend of the series. Table 2 gives the results of the fit for the tidal terms in the weekly, fortnightly, and monthly tidal bands in terms of the amplitude A and phase $\alpha$ of the prograde and retrograde components of the polar motion excitation function defined by:

$$\chi(t) = A_p e^{i\alpha_p} e^{i\phi(t)} + A_r e^{i\alpha_r} e^{-i\phi(t)} \tag{2}$$

where the subscript $p$ denotes prograde, the subscript $r$ denotes retrograde, and $\phi(t)$ represents the tidal argument, the expansion of which is given in Table 1 for the individual tidal terms being considered here. The results at the $Mf'$ and $Mf$ tidal frequencies have been resolved, as have those at the $M9'$ and $M9$ tidal frequencies, with the largest correlation coefficient between the solved-for periodic parameters being 0.024. The results at the semiannual and annual tidal frequencies are not shown since they include such unmodeled, nontidal polar motion excitation effects as seasonal changes in the general thermohaline circulation of the oceans. The uncertainties shown in Table 2 are the 1-sigma formal errors.

Figures 1c and 2c display power spectra of the series obtained by removing the fitted terms from the SPACE94–AAM residual series. As can be seen, there is no longer any evidence of enhanced power in the prograde or retrograde fortnightly tidal bands. Thus, the empirical tide model given in Table 2 can fully account for the enhanced power evident in the SPACE94–AAM residual polar motion excitation series, either in the full series spanning 1976.8–1994 (upon which the fit is based), or in just that portion of the series spanning 1984–1994.

## Comparison with Predictions from Ocean Tide Models

*Seiler [1991]*, using a hydrodynamic ocean tide model, computed the axial and both equatorial components of the angular momentum associated with tidal changes in sea level height and currents for three semidiurnal ($M_2$, $S_2$, $N_2$), three diurnal ($K_1$, $O_1$, $P_1$), and four long-period tides ($Mf'$, $Mf$, $Mm$, $Ssa$). *Gross* [1993] and *Brosche and Wünsch* [1994] used the equatorial components of Seiler's ocean tidal angular momentum results to predict the ocean tidal effect on polar motion. The effects of long-period ocean tides (the sum of the sea level height and current effects) on the polar motion excitation function $\chi(t)$ predicted from Seiler's ocean tidal angular momentum results are computed here by using equation (1) with the tabulated polar motion results of *Gross* [1993a, Table 2] and are given in Table 2 in terms of the amplitude and phase of the prograde and retrograde components.

*Dickman* [1993] developed broadband Liouville equations and used them to predict the Earth rotation effects of 32 short- and long-period ocean tides using tide heights and currents computed from his spherical harmonic ocean tide model [*Dickman*, 1985, 1988b, 1989, 1990a, 1990b, 1991]. The effects of long-period ocean tides (the sum of the sea level height and current terms) on the polar motion excitation function $\chi(t)$ predicted by Dickman's ocean tide model are computed here using equation (1) with the tabulated polar motion results of *Dickman* [1993, Table 3f] and are given in Table 2 in terms of the amplitude and phase of the prograde and retrograde components. (Note that in *Dickman* [1993] the tabulated ocean tidal effects on the prograde and retrograde components of polar motion were inadvertently switched [*Dickman*, personal communication, 1995]. In computing here the predicted effect on the polar motion excitation function, the tabulated prograde polar motion component of *Dickman* [1993, Table 3f] has been interpreted to be, in fact, the retrograde component, and vice versa).

From Table 2, both the Dickman and Seiler ocean tide models predict the greatest long-period ocean tidal effect on the polar motion excitation function to be at the *Mf* tidal frequency. Dickman's model predicts the prograde amplitude to be 1.26 milliarcseconds (mas) and the retrograde amplitude to be 1.72 mas, whereas Seiler's model predicts these amplitudes to be 1.72 mas and 1.44 mas, respectively. Thus, at the *Mf* tidal frequency, the prograde amplitude predicted by Dickman's model is 27 percent smaller than that predicted by Seiler's model, and the retrograde amplitude is 19 percent larger. However, the predicted phases differ by 45° for the prograde component, and 64° for the retrograde component. At the *Mf'* tidal frequency, both models predict the same phases as they predicted at the *Mf* tidal frequency with amplitudes 42 percent as great. Thus, the relative agreement between the Dickman and Seiler model predictions at the *Mf'* tidal frequency is the same as it was at the *Mf* tidal frequency. At the *Mm* tidal frequency, the amplitude for the polar motion excitation function predicted by Dickman's model is substantially smaller than that predicted by Seiler's model, being 0.47 mas for the prograde component (versus 0.78 mas for that predicted by Seiler's model) and 0.28 mas for the retrograde component (versus 0.92 mas for that predicted by Seiler's model). The predicted phases again show large discrepancies of 62° for the prograde component and 35° for the retrograde component. Of the long-period ocean tides considered, the smallest polar motion excitation effects are predicted to occur at the *M9'* tidal frequency, being, 0.13 mas and 0.[illegible] mas for the amplitudes of the prograde and retrograde components, respectively, as predicted by Dickman's ocean tide model.

From Figures 1b and 2b the largest observed effect on the polar motion excitation function is expected to be at the fortnightly tidal frequencies, which is confirmed by the results given in Table 2. At the *Mf* tidal frequency, the observations agree best with the predictions of Dickman's model, with the predicted amplitudes being 47 percent larger for the prograde component and 37 percent smaller for the retrograde component than those observed, but with the phases differing by only 7° for the prograde component and 6° for the retrograde component. The agreement with the observations of the predictions of Seiler's model is substantially worse at the *Mf* tidal frequency than it is with the predictions of Dickman's model, with both prograde and retrograde amplitudes differing from the observations by about a factor of 2, and the prograde and retrograde phases differing by 38° and 58°, respectively.

However, at the *Mf'* tidal frequency, the observations agree better, at least in phase, with the predictions of Seiler's model than they do with the predictions of Dickman's model. The Seiler model predicted prograde and retrograde phases differ from the observations by only 1° and 15°, respectively, although the predicted amplitudes for the prograde component are less than one-half that observed, and for the retrograde component it is less than one-third that observed. Dickman's model predictions at the *Mf'* tidal frequency show greater disagreement with the observations than do Seiler's model predictions, with phases differing by 44° and 79° for the prograde and retrograde components, respectively, the prograde amplitude being less than one-third that observed, and the retrograde amplitude being nearly one-third that observed.

The observed results at the *M9'* and *M9* tidal frequencies are at the level of the formal uncertainty, and Figures 1b and 2b show no evidence of enhanced power in either the prograde or retrograde weekly tidal bands, so there is no evidence for polar motion excitation by these ocean tides. At the *Mm* tidal frequency, the observed effect is somewhat larger than the formal uncertainty, but Figures 1b and 2b again show no evidence of enhanced power in either the prograde or retrograde monthly tidal bands. This indicates that the observed formal uncertainties given in Table 2 may have been underestimated, and inflating them by about a factor of two may give more realistic estimates of the uncertainties. The observed results given in Table 2 for signals at the *M9'*, *M9*, and *Mm* tidal frequencies can be considered to be upper limits on the effect of these ocean tides on the polar motion excitation function $\chi(t)$.

## Discussion

Plots of the spectra of the SPACE94 polar motion excitation series (Figures 1a or 2a) are not symmetric about the zero frequency, but clearly exhibit greater broadband power at retrograde frequencies than at prograde. The asymmetry in the shape of the polar motion excitation spectra is largely eliminated upon removal of the total NCEP AAM series (the sum of the wind and inverted barometer pressure terms) from the SPACE94 polar motion excitation series (compare Figures 1b with 1a, or Figures 2b with 2a). This is strong evidence for broadband excitation of polar motion by atmospheric wind and pressure fluctuations.

Besides removing broadband power, subtracting the total NCEP AAM series from the SPACE94 polar motion excitation series also removes the enhanced power in the prograde weekly tidal band, as mentioned earlier. An examination of Figures 1a and 1b, or Figures 2a and 2b, shows that other peaks in the spectrum of the SPACE94 polar motion excitation series have also been eliminated by removing the NCEP AAM series. Since these peaks appear in spectra computed from different sections of the polar motion excitation time series (compare Figures 1 and 2), they are not likely to arise from statistical fluctuations in the spectral estimation procedure, but more likely indicate that the observed polar motion excitation at these frequencies are also caused by atmospheric fluctuations, perhaps associated with atmospheric Rossby modes.

There have been two other recent attempts to detect long-period ocean tidal excitation of polar motion. *Chao* [1994], using a polar motion excitation series derived from the SPACE93 combination of space-geodetic Earth rotation measurements [*Gross*, 1994], and after first removing the effects of atmospheric wind and pressure fluctuations, found evidence for a 9-day tidal signal as well as a fortnightly tidal amplitude "significantly" greater than that predicted by ocean tide models. *Dickman and Nam* [1995], using the SPACE92 [*Gross*, 1993b] polar motion series without first removing the effects of atmospheric wind and pressure fluctuations, determined prograde and retrograde polar motion amplitudes of 0.061 ± 0.079 mas and 0.063 ± 0.063 mas, respectively, at the fortnightly tidal period, and concluded that at best the SPACE92 polar motion series could be used to place an upper bound on the amplitude of any fortnightly tidal signal. Here, clear evidence for excitation of polar motion at the fortnightly tidal frequencies is obtained by using estimates of the polar motion excitation functions from which the effects of atmospheric wind and pressure fluctuations have been removed.

Predictions from the two available ocean tide models for the effect on the polar motion excitation function $\chi(t)$ of the fortnightly ocean tides agree reasonably well with each other in amplitude (although not in phase). However, except for the prograde *Mf* tidal signal, the predicted amplitudes are considerably smaller than those observed. This indicates that either: (1) both tide models have systematically underestimated the polar motion effect, (2) there are other geophysical mechanisms contributing to the observed effect, or (3) the observed residual polar motion excitation series is contaminated by either measurement noise or errors in the AAM series at the fortnightly tidal frequencies. It is certainly possible, and even probable, that errors exist in both the space-geodetic measurements and the AAM series, especially prior to 1984, although it is difficult to understand why they would be more prominent at the fortnightly tidal frequencies rather than having a more broadband character.

Evidence for either noise contamination or the presence of other geophysical mechanisms also comes from an examination of the recovered prograde and retrograde phases of the *Mf′* and *Mf* tidal signals. If ocean tides were the only cause of the observed fortnightly signals, then the phase of the prograde *Mf'* and *Mf* signals should agree with each other, as should the phases of the retrograde signals [*Dickman,* personal communication, 1995]. From Table 2, the phases of the prograde *Mf'* and *Mf* signals agree with each other to within about 1-sigma, but the retrograde phases do not. One possible additional contributor to the observed fortnightly tidal polar motion excitation signal could be tidal polar motion excitation changes caused by lateral inhomogeneities in the density structure of the crust and mantle, although a quantitative evaluation of this effect must await further investigation.

## Summary

In summary, evidence has been presented for the ocean tidal excitation of polar motion at the *Mf'* (13.63-day) and *Mf* (13.66-day) fortnightly tidal frequencies. Spectra of the polar motion excitation function derived from space-geodetic Earth rotation measurements spanning 1976.8-1994 show enhanced power in the prograde and retrograde fortnightly (14-day) tidal bands, as well as in the prograde weekly (9-day) tidal band (Figures 1a and 2a). Upon subtracting atmospheric wind and pressure effects, spectra of the residual polar motion excitation function continue to exhibit enhanced power in the fortnightly tidal bands, but no longer in the prograde weekly tidal band (Figures 1b and 2b). An empirical model obtained by fitting periodic terms at the tidal frequencies to the SPACE94 - AAM residual polar motion excitation function is able to fully account for this observed enhanced power in the fortnightly tidal bands (Figures 1c and 2c). Predictions from two different ocean tide models generally underestimate the observed fortnightly amplitudes by as much as a factor of two to three (Table 2). At the *Mf* tidal frequency, observations are in best agreement with the predictions of Dickman's ocean tide model, with phases differing by only 6°- 7°, predicted prograde amplitudes being 47 percent too large, and predicted retrograde amplitudes being 37 percent too small. At the *Mf'* tidal frequency, the observed phases are in close agreement with those predicted from Seiler's ocean tide model, differing by only 1° for the prograde component and 15° for the retrograde component; however, Seiler's predicted amplitudes are a factor of two to three times too small. The discrepancies amongst the different model predictions and between the observations and predictions illustrate the need for better models of the effect of long-period ocean tides upon the Earth's rotation, a need that may be fulfilled when long-period ocean tide models based upon Topex/Poseidon measurements become available.

## ACKNOWLEDGMENTS

**Acknowledgments.** One of us (RSG) gratefully acknowledges the assistance given by S. Dickman in helping to understand the predicted Earth rotation effects of his ocean tide model. The work described in this paper was performed at the Jet Propulsion Laboratory, California Institute of Technology, under contract with the National Aeronautics and Space Administration.

# REFERENCES


Barnes, R. T. H., R. Hide, A. A White, and C. A. Wilson, Atmospheric angular momentum fluctuations, length-of-day changes and polar motion, *Proc R Soc. Lond.*, Ser. A, **387,** 31-73, 1983.

Brink, **K. H.,** A laboratory study of open ocean barometric response, *Dyn. Atmos. Oceans*, 2, 153-183, 1978.

Brosche, P., and J. Wünsch, On the "rotational angular momentum" of the oceans and the corresponding polar motion, *Astron. Nachr.*, **315**, 181-188, 1994.

Brosche, P., U. Seiler, J. Sündermann, and J. Wünsch, Periodic changes in Earth's rotation due to oceanic tides, *Astron. Astrophys.*, 220, 318-320, 1989.

Brosche, P., **J.** Wünsch, J. Campbell, and H. Schuh, Ocean tide effects in Universal Time detected by VLBI, *Astron. Astrophys.*, 245, 676-682, 1991.

Brzezinski, A., Polar motion excitation by variations of the effective angular momentum function: considerations concerning deconvolution problem, *manuscripta geodaetica*, **17**, **3-20,** 1992.

Brzezinski, A., and N. Capitaine, The use of the precise observations of the celestial ephemeris pole in the analysis of geophysical excitation of Earth rotation, *J. Geophys. Res.*, **98,** 6667-**6675,** 1993.

Chao, B. F., Excitation of Earth's polar motion by atmospheric angular momentum variations, 1980-1990, *Geophys. Res. Lett.*, 20, 253-256, 1993.

Chao, B. F., Zonal tidal signals in the Earth's polar motion, *Eos Trans. AGU*, 75(44), Fall Meeting Suppl., 158, 1994.

Chao, B. F., R. D. Ray, and G. D. Egbert, Diurnal/semidiurnal oceanic tidal angular momentum: Topex/Poseidon models in comparison with Earth's rotation rate, *Geophys. Res. Lett.*, **22, 1993-1996,** 1995.

Dey, C. H., and L. L. Morone, Evolution of the National Meteorological Center global data assimilation system: January 1982–December 1983, *Mon. Wea. Rev.*, **113**, 304–318, 1985.

Dickman, S. R., The self-consistent dynamic pole tide in global oceans, *Geophys. J. R. atsr. Soc.*, **81**, 157–174, 1985.

Dickman, S. R., Theoretical investigation of the oceanic inverted barometer response, *J. Geophys. Res.*, **93**, 14941–14946, 1988a.

Dickman, S. R., The self-consistent dynamic pole tide in non-global oceans, *Geophys. J. Int.*, **94**, 519–543, 1988b.

Dickman, S. R., A complete spherical harmonic approach to luni-solar tides, *Geophys. J. Int.*, **99**, 457–468, 1989.

Dickman, S. R., Corrigendum, *Geophys. J. Int.*, **102**, 265, 1990a.

Dickman, S. R., Experiments in tidal mass conservation, *Geophys. J. Int.*, **102**, 257–262, 1990b.

Dickman, S. R., Ocean tides for satellite geodesy, *Mar. Geod.*, **14**, 21–56, 1991.

Dickman, S. R., Dynamic ocean-tide effects on Earth's rotation, *Geophys. J. Int.*, **112**, 448–470, 1993.

Dickman, S. R., and Y. S. Nam, Revised predictions of long-period ocean tidal effects on Earth's rotation rate, *J. Geophys. Res.*, **100**, 8233–8243, 1995.

Eubanks, T. M., Variations in the orientation of the Earth, in *Contributions of Space Geodesy to Geodynamics: Earth Dynamics*, edited by D. E. Smith, and D. L. Turcotte, pp. 1–54, American Geophysical Union Geodynamics Series, Washington, D.C., 1993.

Eubanks, T. M., J. A. Steppe, J. O. Dickey, R. D. Rosen, and D. A. Salstein, Causes of rapid motions of the Earth's pole, *Nature*, 334, 115–119, 1988.

Freedman, A. P., R. Ibañez-Meier, T. A. Herring, S. M. Lichten, and J. O. Dickey, Subdaily Earth rotation during the Epoch '92 campaign, *Geophys. Res. Lett.*, **21**, 769–772, 1994a.

Freedman, A. P., J. A. Steppe, J. O. Dickey, T. M. Eubanks, and L. Y. Sung, The short-term prediction of universal time and length of day using atmospheric angular momentum, *J. Geophys. Res.*, **99**, 6981-6996, 1994b.

Fu, L.-L., and G. Pihos, Determining the response of sea level to atmospheric pressure forcing using TOPEX/POSEIDON data, *J. Geophys. Res.*, **99**, 24633-24642, 1994.

Gross, R. S., Correspondence between theory and observations of polar motion, *Geophys. J. Int.*, **109**, 162-170, 1992.

Gross, R. S., The effect of ocean tides on the Earth's rotation as predicted by the results of an ocean tide model, *Geophys. Res. Lett.*, **20**, 293-296, 1993a.

Gross, R. S., A combination of Earth orientation data: SPACE92, in *IERS Technical Note 14: Earth Orientation, Reference Frames and Atmospheric Excitation Functions Submitted for the 1992 IERS Annual Report*, edited by P. Charlot, pp. C1-C8, Observatoire de Paris, Paris, France, 1993b.

Gross, R. S., A combination of Earth orientation data: SPACE93, in *IERS Technical Note 17: Earth Orientation, Reference Frames and Atmospheric Excitation Functions Submitted for the 1993 IERS Annual Report*, edited by P. Charlot, pp. C5-C12, Observatoire de Paris, Paris, France, 1994.

Gross, R. S., A combination of EOP measurements: SPACE94, in *IERS Technical Note 19: Earth Orientation, Reference Frames and Atmospheric Excitation Functions Submitted for the 1994 IERS Annual Report*, edited by P. Charlot, in press, Observatoire de Paris, Paris, France, 1995.

Gross, R. S., and U. J. Lindqwister, Atmospheric excitation of polar motion during the GIG '91 measurement campaign, *Geophys. Res. Lett.*, **19**, 849-852, 1992a.

Gross, R. S., and U. J. Lindqwister, Comparison of GIG '91 polar motion results with atmospheric angular momentum chi functions, in *Proceedings of the Sixth International Geodetic Symposium on Satellite Positioning*, Columbus, Ohio, March 17-20, 1992b.

Herring, T. A., Diurnal and semidiurnal variations in Earth rotation, in *Observations of Earth from Space*, edited by R. P. Singh, M. Feissel, B. D. Tapley, and C. K. Shum, *Adv. Space Res.*, **13**, (11)281-(11)290, Pergamon, Oxford, 1993.

Herring, T. A., and D. Dong, Current and future accuracy of Earth rotation measurements, in *Proceedings of the AGU Chapman Conference on Geodetic VLBI: Monitoring Global Change*, edited by W. E. Carter, pp. 306-324, NOAA Technical Report NOS 137 NGS 49, Washington, D.C., 1991.

Herring, T. A., and D. Dong, Measurement of diurnal and semidiurnal rotational variations and tidal parameters of Earth, *J. Geophys. Res.*, **99**, 18051-18071, 1994.

Kalnay, E., M. Kanamitsu, and W. E. Baker, Global numerical weather prediction at the National Meteorological Center, *Bull. Amer. Met. Soc.*, **71**, 1410-1428, 1990.

Kanamitsu, M., Description of the NMC global data assimilation and forecast system, *Wea. and Forecasting*, **4**, 335-342, 1989.

Kistler, R. E., and D. F. Parrish, Evolution of the NMC data assimilation system: September 1978–January 1982, *Mon. Wea. Rev.*, **110**, 1335-1346, 1982.

Kosek, W., J. Nastula, and B. Kolaczek, Variability of polar motion oscillations with periods from 20 to 150 days in 1979-1991, *Bull. Géod.*, **69**, 308-319, 1995.

Kuehne, J., S. Johnson, and C. R. Wilson, Atmospheric excitation of nonseasonal polar motion, *J. Geophys. Res.*, **98**, 19973-19978, 1993.

Lambeck, K., *The Earth's Variable Rotation: Geophysical Causes and Consequences*, 449 pp., Cambridge University Press, New York, 1980.

Lambeck, K., *Geophysical Geodesy: The Slow Deformations of the Earth*, 718 pp., Oxford University Press, Oxford, 1988.

Lichten, S. M., S. L. Marcus, and J. O. Dickey, Sub-daily resolution of Earth rotation variations with Global Positioning System measurements, *Geophys. Res. Lett.*, **19**, 537-540, 1992.

McPherson, R. D., K. H. Bergman, R. E. Kistler, G. E. Rasch, and D. S. Gordon, The NMC operational global data assimilation system, *Mon. Wea. Rev.*, **107**, 1445-1461, 1979.

Morabito, D. D., T. M. Eubanks, and J. A. Steppe, Kalman filtering of Earth orientation changes, in *The Earth's Rotation and Reference Frames for Geodesy and Geodynamics*, edited by A. K. Babcock and G. A. Wilkins, pp. 257-267, D. Reidel, Dordrecht, Holland, 1988.

Moritz, H., and I. I. Mueller, *Earth Rotation: Theory and Observation*, 617 pp., Ungar, New York, 1988.

Munk, W. H., and G. J. F. MacDonald, *The Rotation of the Earth: A Geophysical Discussion*, 323 pp., Cambridge University Press, New York, 1960.

Nastula, J., Short periodic variations in the Earth's rotation in the period 1984--1990, *Ann. Geophysicae*, **10**, 441-448, 1992.

Nastula, J., Short periodic variations of polar motion and hemispheric atmospheric angular momentum exzcitation functions in the period 1984-1992, *Ann. Geophysicae*, **13**, 217-225, 1995.

Nastula, J., D. Gambis, and M. Feissel, Correlated high frequency variations in polar motion and of the length of the day in early 1988, *Ann. Geophysicae*, **8**, 565-570, 1990.

Ponte, R. M., The sea level response of a stratified ocean to barometric pressure forcing, *J. Phys. Oceanogr.*, **22**, 109-113, 1992.

Ponte, R. M., Variability in a homogenous global ocean forced by barometric pressure, *Dyn. Atmos. Oceans*, **18**, 209-234, 1993.

Ponte, R. M., Understanding the relation between wind- and pressure-driven sea level variability, *J. Geophys. Res.*, **99**, 8033-8039, 1994.

Ponte, R. M., D. A. Salstein, and R. D. Rosen, Sea level response to pressure forcing in a barotropic numerical model, *J. Phys. Oceanogr.*, **21**, 1043-1057, 1991.

Ray, R. D., D. J. Steinberg, B. F. Chao, and D. E. Cartwright, Diurnal and semidiurnal variations in the Earth's rotation rate induced by oceanic tides, *Science*, **264**, 830-832, 1994.

Salstein, D. A., and R. D. Rosen, Regional contributions to the atmospheric excitation of rapid polar motions, *J. Geophys. Res.*, **94**, 9971-9978, 1989

Salstein, D. A., D. M. Kann, A. J. Miller, and R. D. Rosen, The Sub-Bureau for Atmospheric Angular Momentum of the International Earth Rotation Service: A meteorological data center with geodetic applications, *Bull. Amer. Meteorol. Soc.*, **74**, 67-80, 1993.

Seiler, U., Periodic changes of the angular momentum budget due to the tides of the world ocean, *J. Geophys. Res.*, **96**, 10287-10300, 1991.

Sovers, O. J., C. S. Jacobs, and R. S. Gross, Measuring rapid ocean tidal Earth orientation variations with VLBI, *J. Geophys. Res.*, **98**, 19959-19971, 1993.

Tai, C.-K., On the quasigeostrophic oceanic response to atmospheric pressure forcing: The inverted barometer pumping, *NOAA Tech. Memo. NOS OES 005*, 19 pp., Nat. Oceanic and Atmos. Admin. Nat. Ocean Serv., Rockville, Md., 1993.

Watkins, M. M., and R. J. Eanes, Diurnal and semidiurnal variations in Earth orientation determined from LAGEOS laser ranging, *J. Geophys. Res.*, **99**, 18073-18079, 1994.

Wunsch, C., Bermuda sea level in relation to tides, weather, and baroclinic fluctuations, *Rev. Geophys.*, **10**, 1-49, 1972.

Wunsch, C., Large-scale response of the ocean to atmospheric forcing at low frequencies, *J. Geophys. Res.*, **96**, 15083-15092, 1991.

Wünsch, J., and J. Busshoff, Improved observations of periodic UT1 variations caused by ocean tides, *Astron. Astrophys.*, **266**, 588-591, 1992.

Wünsch, J., and U. Seiler, Theoretical amplitudes and phases of the periodic polar motion terms caused by ocean tides, *Astron. Astrophys.*, **266**, 581-587, 1992.

Yoder, C. F., J. G. Williams, and M. E. Parke, Tidal variations of Earth rotation, *J. Geophys. Res.*, **86**, 881-891, 1981.

## FIGURE CAPTIONS

Fig. 1. Power spectral density (psd) estimates in decibels (db) computed from time series of polar motion excitation functions $\chi(t)$ spanning 1976.8-1994 of: (a) the SPACE94 polar motion excitation function derived from space-geodetic Earth rotation measurements, (b) the residual polar motion excitation function formed by subtracting the AAM series shown in Figure 3 from the SPACE94 excitation **series,** and **(c)** the result of removing the recovered tidal terms from the SPACE94 **AAM** residual series. The vertical dotted lines indicate frequencies in the prograde and retrograde weekly tidal bands (at $\pm$40.01 cpy), fortnightly tidal bands (at $\pm$ 26.74 cpy), and monthly tidal bands (at $\pm$13.26 cpy). The retrograde component of polar motion excitation is represented by negative frequencies, the prograde component by positive frequencies.

Fig. 2. As in Figure 1 but for the time span of 1984-1994.

Fig. 3. The x-component (a) and y-component (b) of the effective atmospheric angular momentum chi-function computed from the NCEP atmospheric wind and pressure fields. The effective AAM chi-functions displayed here are the sum of the wind term and the pressure term computed under the inverted barometer assumption for the response of the oceans to the imposed atmospheric pressure fluctuations.

Table 1. Expansion of the Tidal Argument

| Tide | Period (solar days) | Fundamental Argument $l$ | $l'$ | $F$ | $D$ | $\Omega$ |
|---|---|---|---|---|---|---|
| Weekly | | | | | | |
| *M9'* | 9.12 | 1 | 0 | 2 | 0 | 1 |
| *M9* | 9.13 | 1 | 0 | 2 | 0 | 2 |
| Fortnightly | | | | | | |
| *Mf'* | 13.63 | 0 | 0 | 2 | 0 | 1 |
| *Mf* | 13.66 | 0 | 0 | 2 | 0 | 2 |
| Monthly | | | | | | |
| *Mm* | 27.55 | 1 | 0 | 0 | 0 | 0 |
| Semiannual | | | | | | |
| *Ssa* | 182.62 | 0 | 0 | 2 | 2 | 2 |
| Annual | | | | | | |
| *Sa* | 365.26 | 0 | 1 | 0 | 0 | 0 |

Table 2. Observed and Predicted Effects of Long-Period Ocean Tides on the Polar Motion Excitation Function $\chi(t)$

| | Prograde Amplitude (mas) | Prograde Phase (degrees) | Retrograde Amplitude (mas) | Retrograde Phase (degrees) |
|---|---|---|---|---|
| *M9'* (9.12-day) | | | | |
| SPACE94 AAM | 0.54 ± 0.45 | 38 ± 48 | 0.21 ± 0.45 | 79 ± 126 |
| Dickman | 0.13 | 73 | 0.21 | 15 |
| *M9* (9.13-day) | | | | |
| SPACE94 AAM | 0.47 ± 0.45 | 30 ± 55 | 0.41 ± 0.45 | 95 ± 63 |
| Dickman | 0.32 | 73 | 0.52 | 15 |
| *Mf'* (13.63-day) | | | | |
| SPACE94 AAM | 1.01 ± 0.45 | 56 ± 16 | 2.01 ± 0.45 | 87 ± 13 |
| Dickman | 0.52 | 100 | 0.71 | 8 |
| Seiler/Gross | 0.72 | 55 | 0.59 | 72 |
| *Mf* (13.66-day) | | | | |
| SPACE94 AAM | 0.86 ± 0.45 | 93 ± 30 | 2.73 ± 0.45 | 14 ± 10 |
| Dickman | 1.26 | 100 | 1.72 | 8 |
| Seiler/Gross | 1.72 | 55 | 1.44 | 72 |
| *Mm* (27.55-day) | | | | |
| SPACE94 AAM | 0.75 ± 0.45 | 49 ± 35 | 0.82 ± 0.45 | -59 ± 32 |
| Dickman | 0.47 | 136 | 0.28 | -7 |
| Seiler/Gross | 0.78 | 74 | 0.92 | 28 |

POLAR MOTION EXCITATION SPECTRA (1976.8- 1994)

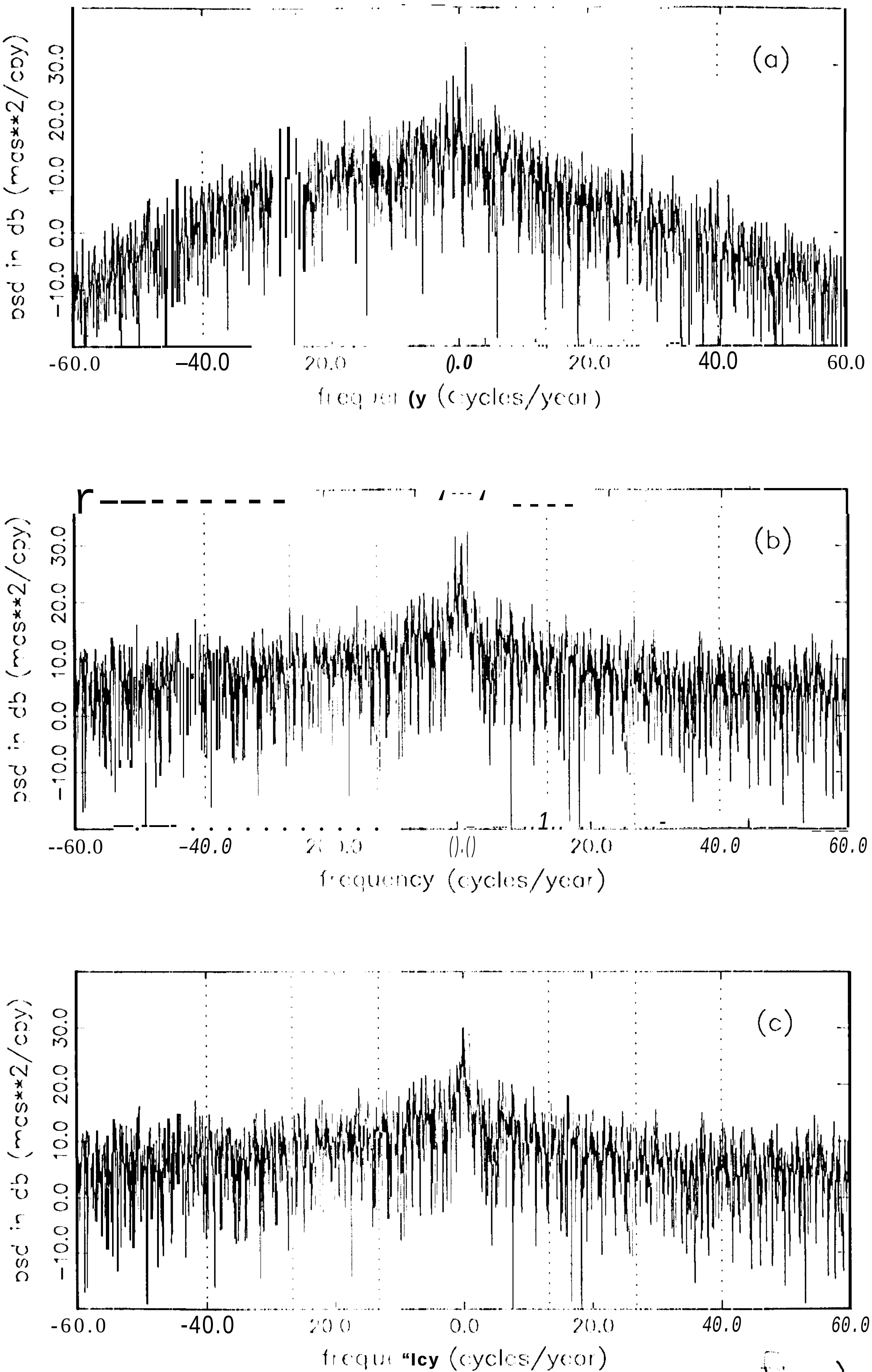


Fig. 1

POLAR MOTION EXCITATION SPECTRA (1984--1994)

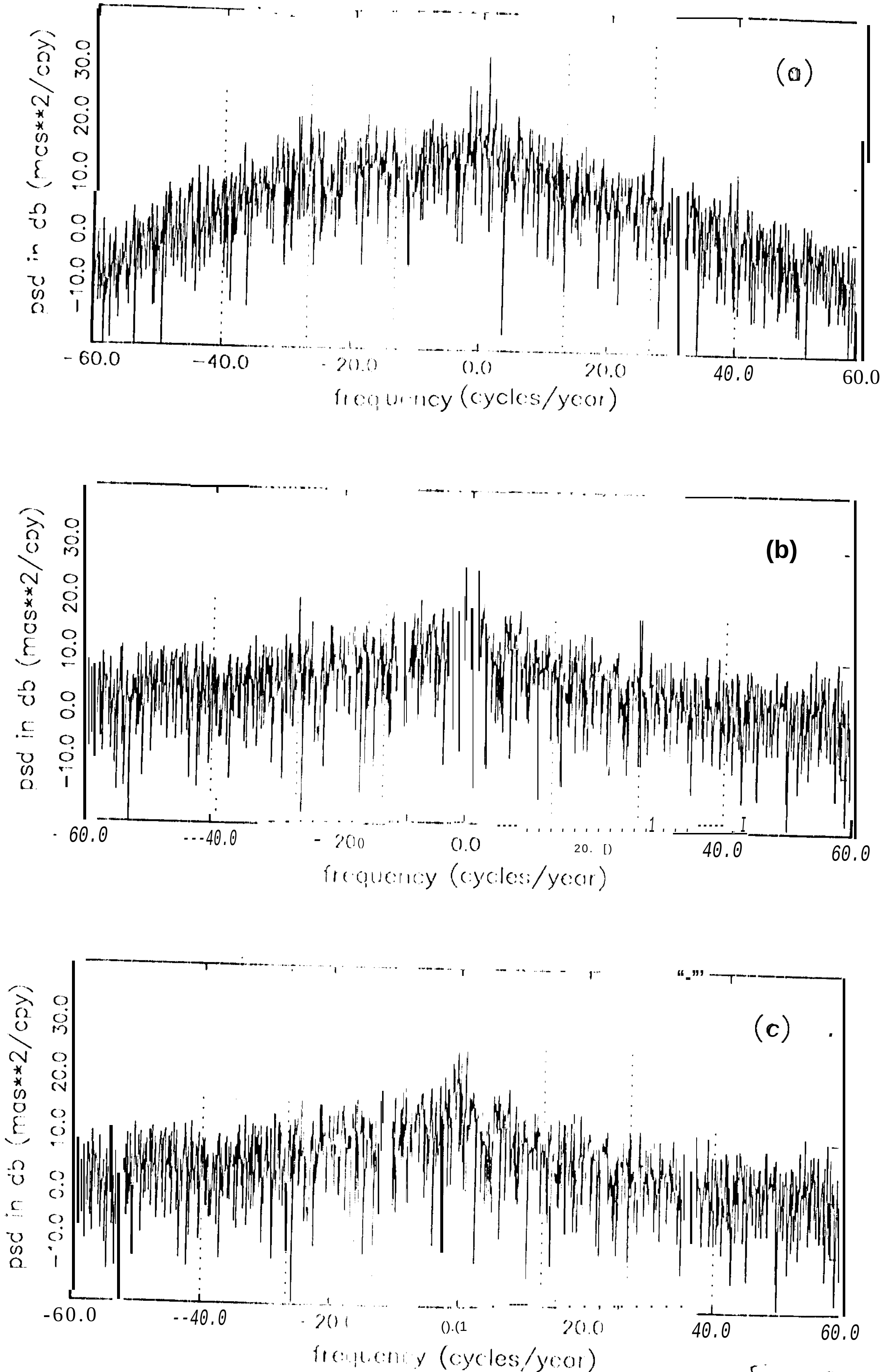


Fig. 2

EFFECTIVE ATMOSPHERIC ANGULAR MOMENTUM

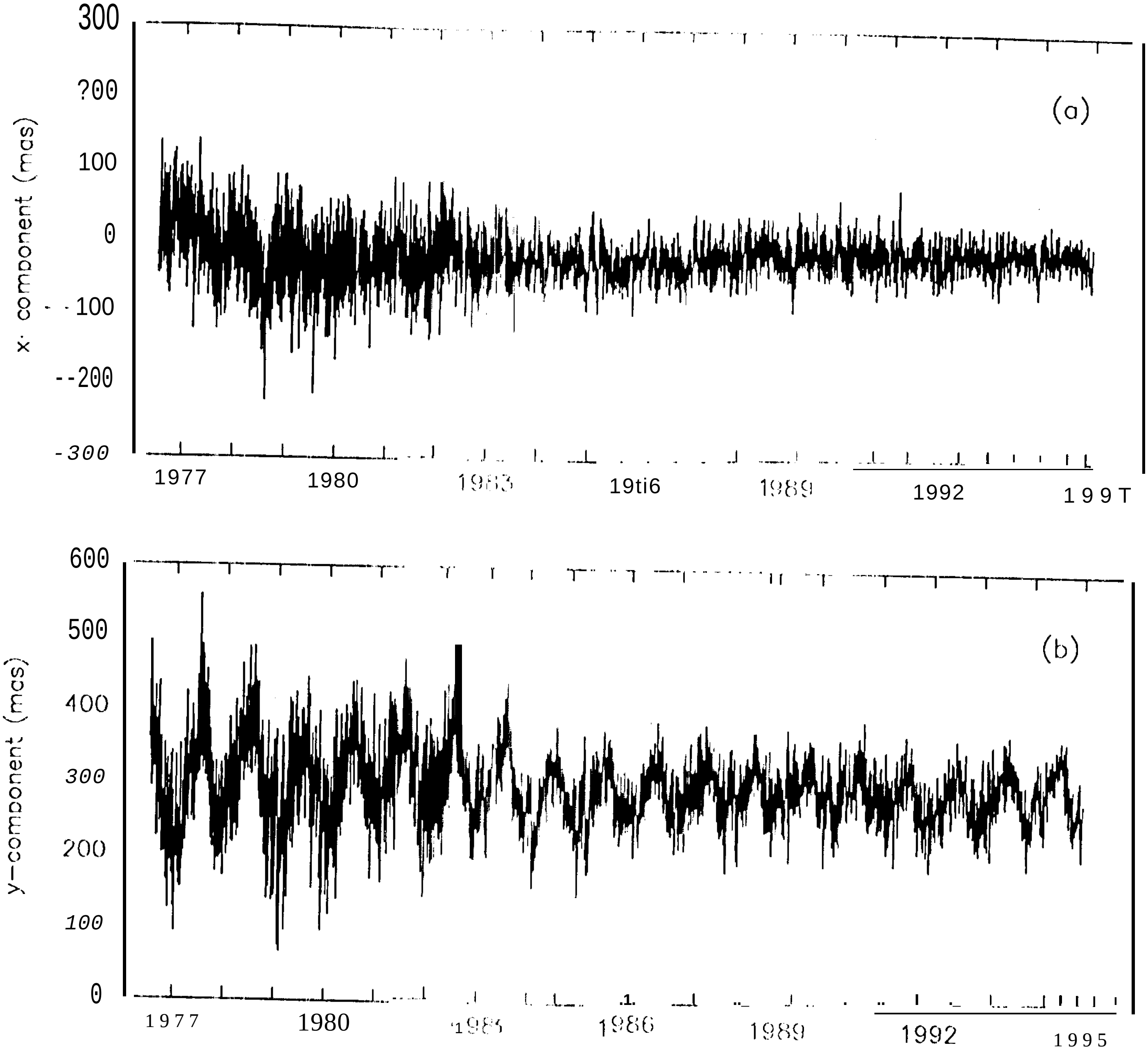


Fig. 3